

Clustering of surface NMDA receptors is mainly mediated by the C-terminus of GluN2A in cultured rat hippocampal neurons

Ying-Gang Yan, Jie Zhang, Shu-Jun Xu, Jian-Hong Luo, Shuang Qiu, Wei Wang[#]

Department of Neurobiology, Key Laboratory of Medical Neurobiology of the Ministry of Health of China, Zhejiang Province Key Laboratory of Neurobiology, Zhejiang University School of Medicine, Hangzhou 310058, China

[#]Current affiliation: School of Nano-Bioscience and Chemical Engineering, Ulsan National Institute of Science and Technology, Ulsan 689-798, South Korea

Corresponding authors: Shuang Qiu and Wei Wang. E-mail: qiushly@zju.edu.cn, weiwang31@unist.ac.kr

© Shanghai Institutes for Biological Sciences, CAS and Springer-Verlag Berlin Heidelberg 2014

ABSTRACT

N-methyl-D-aspartate receptors (NMDARs) containing different GluN2 subunits play distinct roles in synaptic plasticity. Such differences may not only be determined by the channel properties, but also by differential surface distribution and synaptic localization. In the present study, using a Cy3-conjugated Fab fragment of the GFP antibody to label surface-located GluN2 subunits tagged with GFP at the N-terminus, we observed the membrane distribution patterns of GluN2A- or GluN2B-containing NMDARs in cultured rat hippocampal neurons. We found that surface NMDARs containing GluN2A, but not those containing GluN2B, were inclined to cluster at DIV7. Swapping the carboxyl termini of the GluN2 subunits completely reversed these distribution patterns. In addition, surface NMDARs containing GluN2A were preferentially associated with PSD-95. Taken together, the results of our study suggest that the clustering distribution of GluN2A-containing NMDARs is determined by the GluN2A C-terminus, and its interaction with PSD-95 plays an important role in this process.

Keywords: NMDA receptors; GluN2A; GluN2B; PSD-95; receptor clustering

INTRODUCTION

N-methyl-D-aspartate-type ionotropic glutamate receptors

(NMDARs) in the central nervous system play critical roles in synaptic plasticity, synaptogenesis, and excitotoxicity^[1,2,3]. Functional NMDARs are believed to be tetrameric complexes assembled from two GluN1 and two GluN2 (GluN2A–2D) subunits^[4,5]. Different NMDAR subtypes have distinct channel properties, such as open probability and time-course of currents^[6]. Moreover, the surface expression and synaptic localization of different NMDAR subtypes are distinct and differentially regulated during development and in response to neuronal activity and sensory experience. At nascent synapses, NMDARs predominantly contain GluN2B. During postnatal development, there is an increase in the expression and subsequent surface localization of GluN2A-containing NMDARs^[7]. Neuronal activity may bidirectionally remodel the synaptic localization of NMDAR subtypes. Chronic activity enhances the levels of GluN2A-containing NMDARs at synaptic sites, while blockade of activity promotes the surface expression of those containing GluN2B^[8].

The GluN2 subunit plays critical roles in controlling the surface expression and synaptic localization of NMDARs. It has an intracellular C-terminus which may interact directly with other scaffolding proteins, adaptor proteins, or downstream signaling proteins. The PDZ-binding motif at the distal end of the C-terminus directly interacts with PSD-MAGUK proteins, such as PSD-95 and SAP102^[9,10] and this interaction promotes NMDAR clustering^[11], surface expression^[12], and the targeting of GluN2A *versus* GluN2B to synapses^[13]. Furthermore, the C-terminus of the

GluN2 subunit contains several sites for post-translational modification such as phosphorylation and palmitoylation, which may contribute to the distinct regulation of NMDAR subtypes^[14].

In this study, by imaging surface NMDARs using a Cy3-conjugated Fab fragment of GFP antibody, we found that the GluN2A-containing NMDARs were more clustered, while those containing GluN2B were more diffuse in both immature and mature hippocampal neurons. And the clustering distribution of the GluN2A-containing NMDARs was determined by the subunit C-terminus.

MATERIALS AND METHODS

DNA Constructs

Construction of EGFP-GluN2B, EGFP-GluN2A, ECFP-GluN2A, and ECFP-GluN2B was as described previously^[5,15]. GFP or CFP was tagged to GluN2B or GluN2A at the extracellular N-terminus. EGFP-PSD-95 and EGFP-SAP102 were gifts from S. Visini (Georgetown University, Washington, DC). To generate the GFP-GluN2A- Δ 7 or CFP-GluN2A- Δ 7 construct, the first two primers, (5'-TG TAGCGATGTTGACCGCACCTACA-3' and 5'-AGGCAGATCTTACTTGTACTCGTCTATTGCTGCAGG-3'), were designed and used in PCR cloning of the cDNA sequence encoding the C-terminal tail of GluN2A lacking the PDZ binding domain (PSIESDV)^[9], using the original EGFP-GluN2A or ECFP-GluN2A construct as template. Then the BglII-treated original GFP-GluN2A or CFP-GluN2A construct and the PCR fragments were ligated with T4 ligase. The construction of GFP/CFP-GluN2A-Mut3 was similar to that of GFP/CFP-GluN2A- Δ 7 and subcloned with PCR products encoding the C-terminal tail of GluN2A which had 11 amino acids identical to GluN2B. GFP/CFP-GluN2B-C_{GluN2A} was constructed to replace the complete C-terminal of GFP/CFP-GluN2B with the complete C-terminal of GluN2A. GFP/CFP-GluN2A-C_{GluN2B} was constructed to replace the complete C-terminal of GFP/CFP-GluN2A with that of GluN2B. All constructs were verified by DNA sequencing.

Neuron Culture and Transfection

Primary hippocampal cultures were prepared from one-day postnatal Sprague-Dawley rats as described previously^[15]. Briefly, the hippocampi were chopped and

digested in 0.25% trypsin (Sigma, St. Louis, MO) for 15 min at 37°C. Dissociated cells were plated at a density of 1×10^6 in 35-mm dishes with poly-L-lysine-coated coverslips in Dulbecco's modified Eagle's medium (DMEM; Invitrogen, Carlsbad, CA) containing 10% fetal bovine serum (FBS), 10% horse serum, and 2 mmol/L glutamine (all from Invitrogen). The culture medium was changed to Neurobasal medium plus B27 (Invitrogen) the next day. The neurons were routinely transfected after 5 days *in vitro* (DIV5) by adding 3 to 4.5 μ g of total DNA and 4 μ L Lipofectamine 2000 (Invitrogen) in a final volume of 500 μ L OPTI-MEM to the 35-mm dish containing neurons and 1.5 mL Neurobasal medium, and incubated for 3 h at 37°C. The cells were then rinsed in Neurobasal medium and the original medium was added.

Generation of Cy3-conjugated Anti-GFP Fab Fragment

Glutathione S-transferase (GST) and histamine (HIS) fusion GFP proteins were cloned, expressed, and purified using conventional methods. A polyclonal antibody to GFP was generated by immunizing rabbits with GST-GFP fusion protein, then affinity-purified on nitrocellulose strips containing the HIS-GFP fusion protein. The Fab fragment was generated by papain cleavage of anti-GFP polyclonal antibodies. The Fab fragment was conjugated to the Cy3 fluorophore with the Cy3 mAb labelling kit following the manufacturer's instructions (Amersham Biosciences, Piscataway, NJ). The purity of the Fab fragment was confirmed by SDS-PAGE.

Surface Staining and Immunocytochemistry

Anti-GFP surface staining was performed as previously described^[15]. Briefly, coverslips were incubated with rabbit polyclonal antibody against GFP for 7 min at room temperature, then, after washes, neurons were incubated with Alexa546-conjugated goat anti-rabbit antibody (Molecular Probes, Grand island, NY) for another 7 min at room temperature, then viewed directly under a fluorescence microscope. For anti-GFP Fab surface staining, transfected neurons were incubated only with Cy3-conjugated anti-GFP Fab fragment at 2 μ g/mL for 8 min at room temperature before imaging.

For immunocytochemical studies, neurons were fixed with 4% paraformaldehyde, washed with PBS, permeabilized with 0.2% Triton X-100/PBS, blocked with

10% normal goat serum in PBS for 30 min, washed with PBS, incubated with primary antibody for 1 h at room temperature, and stained with Alexa Fluor 488 goat anti-mouse secondary antibody (Molecular Probes, Grand Island, NY) for 1 h at room temperature. Anti-PSD-95 antibody (Upstate Biotechnology, Lake Placid, NY) was used at 1:200 dilution, and anti-synaptophysin antibody (Abcam, Cambridge, MA) was used at 1:200 dilution.

Image Acquisition and Data Analysis

Neurons that appeared healthy and morphologically intact were imaged by fluorescence microscopy. Fluorescent labeling was imaged with an Olympus FLUO1000 confocal microscope (Tokyo, Japan) with a 40× PlanApo oil-immersion objective (0.65 NA). Images for each fluorophore were acquired sequentially and averaged over three scans. The image data were analyzed and quantified using MetaMorph software (Universal Imaging Corp., West Chester, PA). For surface receptor analysis, clusters were determined by a threshold set at twice the average dendritic gray value, and the number of clusters from at least 5 dendrites extending at least 100 μm was measured. Average total intensity per 10 μm of surface staining was analyzed with MetaMorph software. Five dendritic sections were measured and averaged to give a value for each cell included. Co-localization with PSD-95, SAP102, and synaptophysin was defined as having overlapping or adjacent pixels. All data were analyzed using SPSS version 13 (SPSS, Chicago, IL). Statistics were calculated with Student's *t* test, and significance was set at *P* < 0.05. Data are expressed as mean ± SEM.

RESULTS

Distribution Pattern of Surface NMDARs in Cultured Hippocampal Neurons during Development

To explore the distribution patterns of surface NMDARs, we transfected GFP-tagged GluN2 plasmids (GFP-GluN2A or GFP-GluN2B) into cultured hippocampal neurons. Since GFP labeled the N-terminus of the GluN2 subunit, live cell-surface staining with anti-GFP antibody was used to detect the surface GFP-GluN2 subunits at different times after transfection^[15]. To exclude the cascade reaction of primary and secondary antibodies and shorten the staining time, we generated a Cy3-conjugated Fab fragment of GFP antibody

(Fab-Cy3) for surface staining of the GFP-GluN2 subunits. We found that, at DIV7, more clusters were observed when surface GFP-GluN2B was stained with polyclonal anti-GFP antibody (Fig. 1A, upper panels) compared with Fab-Cy3 staining (Fig. 1A, lower panels). This indicated that the cascade reaction of primary and secondary antibodies and a longer staining time may induce clustering of surface receptors. Therefore, we used Fab-Cy3 in the subsequent experiments, rather than polyclonal anti-GFP antibody, to assess the distribution pattern of surface GFP-GluN2.

To ensure comparability of surface staining, equal amounts of GFP-GluN2B or GFP-GluN2A cDNA were transfected into cultured hippocampal neurons at DIV5. First, we observed the distribution patterns of the surface GFP-GluN2B and GFP-GluN2A 2 days after transfection (DIV7) and found that most of the surface GFP-GluN2B was diffusely distributed throughout the soma and dendrites with rare clusters (Fig. 1B, upper panels). In contrast, the surface GFP-GluN2A was distributed in a clustered pattern. Quantitative analysis showed that the density of surface GFP-GluN2A clusters was statistically higher than that of GFP-GluN2B clusters (Fig. 1C). These results indicated that the surface distribution pattern of NMDARs containing GluN2B is distinct from those containing GluN2A during the early stage of hippocampal neuron development. Then, we assessed the synaptic localization of surface GFP-GluN2A clusters and found that, at DIV7, the density of clusters of synaptophysin, a presynaptic marker, was much lower than that of surface GFP-GluN2A clusters, although most of synaptophysin was co-localized with GFP-GluN2A. This indicated that the surface GFP-GluN2A clusters were located not only in the synapses, but also in the dendritic shaft and soma (Fig. 1D).

Next, we examined the surface distribution of GFP-GluN2A and GFP-GluN2B at DIV14 and found that, although the density of surface GFP-GluN2B clusters increased significantly (Fig. 2A, upper panels), it was still statistically lower than that of surface GFP-GluN2A clusters (Fig. 2A, lower panels). We further analyzed the ratio of average immunofluorescence intensity between clustered receptors and diffuse receptors, and found that this ratio for GFP-GluN2A was statistically higher than that for GFP-GluN2B. These results indicated that surface NMDARs containing GluN2A form more clusters than those containing GluN2B in mature hippocampal neurons.

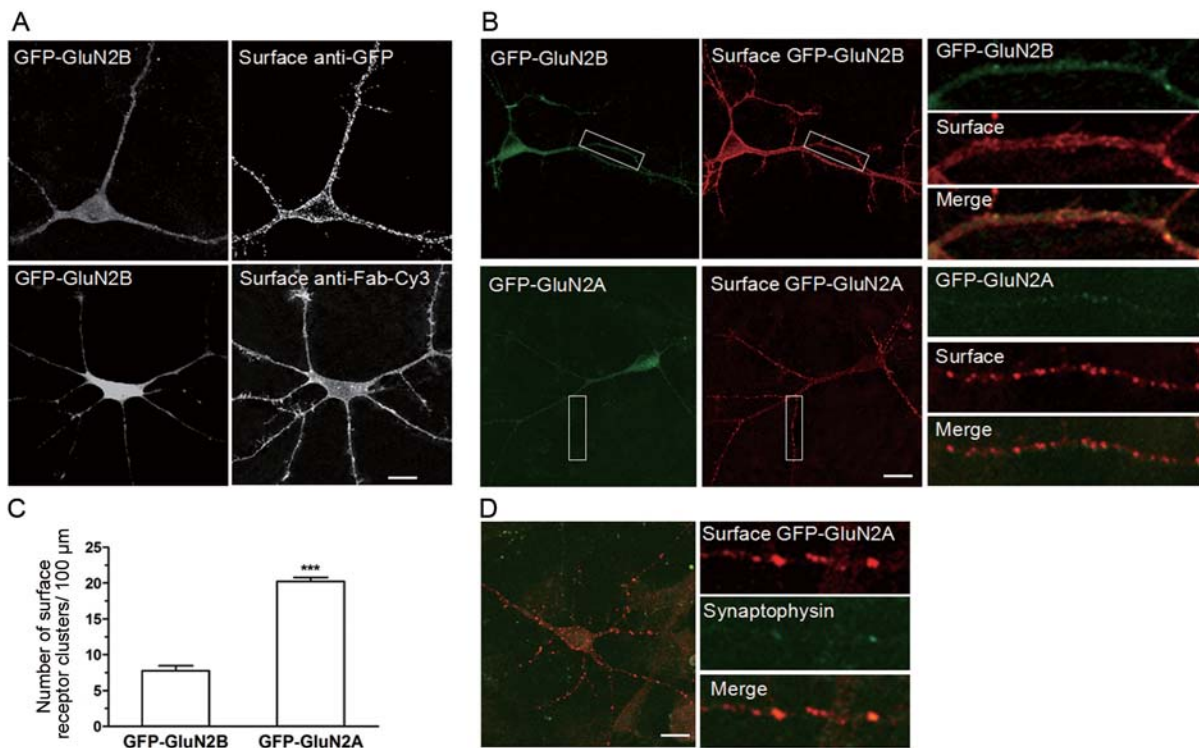


Fig. 1. Surface NMDARs containing GluN2A are more inclined to cluster than those containing GluN2B at DIV7. **A:** GFP-tagged GluN2B construct was transfected into cultured hippocampal neurons at DIV5. Then surface-expressed receptors were detected at DIV7 by conventional anti-GFP antibody (upper panels) or Cy3-conjugated anti-GFP antibody Fab fragment (Fab-Cy3, lower panels) (scale bar, 10 μm). **B:** Live cultured hippocampal neurons transfected with GFP-GluN2A or GFP-GluN2B at DIV5 were surface-stained with Fab-Cy3 at DIV7 (scale bar, 10 μm). In each panel, insets show segments of dendrites with GFP-GluN2 fluorescence (green), surface staining with Cy3-conjugated anti-GFP Fab (red), and their merged images. **C:** Quantitative analysis of the number of surface-distributed GluN2A-containing or GluN2B-containing NMDAR clusters per 100 μm dendrite at DIV7 after transfection with GFP-GluN2A or GFP-GluN2B at DIV5 (***) $P < 0.01$, Student's *t* test; error bars represent mean \pm SEM). **D:** Co-localization of surface GluN2A-NMDAR clusters (red) with the presynaptic marker synaptophysin (green) at DIV7 after transfection with GFP-GluN2A at DIV5 (scale bar, 10 μm).

In addition, the surface GFP-GluN2A clusters partially co-localized with synaptophysin at DIV14 (Fig. 2D). Taken together, our data suggested that, compared with surface NMDARs containing GluN2B, those containing GluN2A are more inclined to cluster in both premature and mature hippocampal neurons.

The C-Terminus of the GluN2 Subunit Determines the Distribution Pattern of Surface NMDARs

The GluN2 subunit has a long, intracellular C-terminus which mediates the intracellular trafficking and synaptic targeting of NMDARs^[16,17]. To assess whether it contributes to the distribution patterns of surface NMDARs, we constructed the chimeric mutants GFP-GluN2B-C_{GluN2A} and

GFP-GluN2A-C_{GluN2B}, in which the C-termini of GluN2A and GluN2B were completely exchanged (Fig. 3A). We found that the surface density of GFP-GluN2B-C_{GluN2A} clusters at DIV7 was significantly increased and did not statistically differ from that of GFP-GluN2A clusters (Fig. 3B). In contrast, the surface GFP-GluN2A-C_{GluN2B} was distributed in a more diffuse pattern, similar to that of GFP-GluN2B. The surface density of GFP-GluN2A-C_{GluN2B} clusters was significantly lower than that of GFP-GluN2A. These results indicated that the surface distribution pattern of NMDARs depends on the C-terminus of GluN2.

The last four amino-acids (ESDV) of GluN2 form the PDZ-binding domain, which directly interacts with proteins of the PSD-MAGUK family and mediates the clustering and

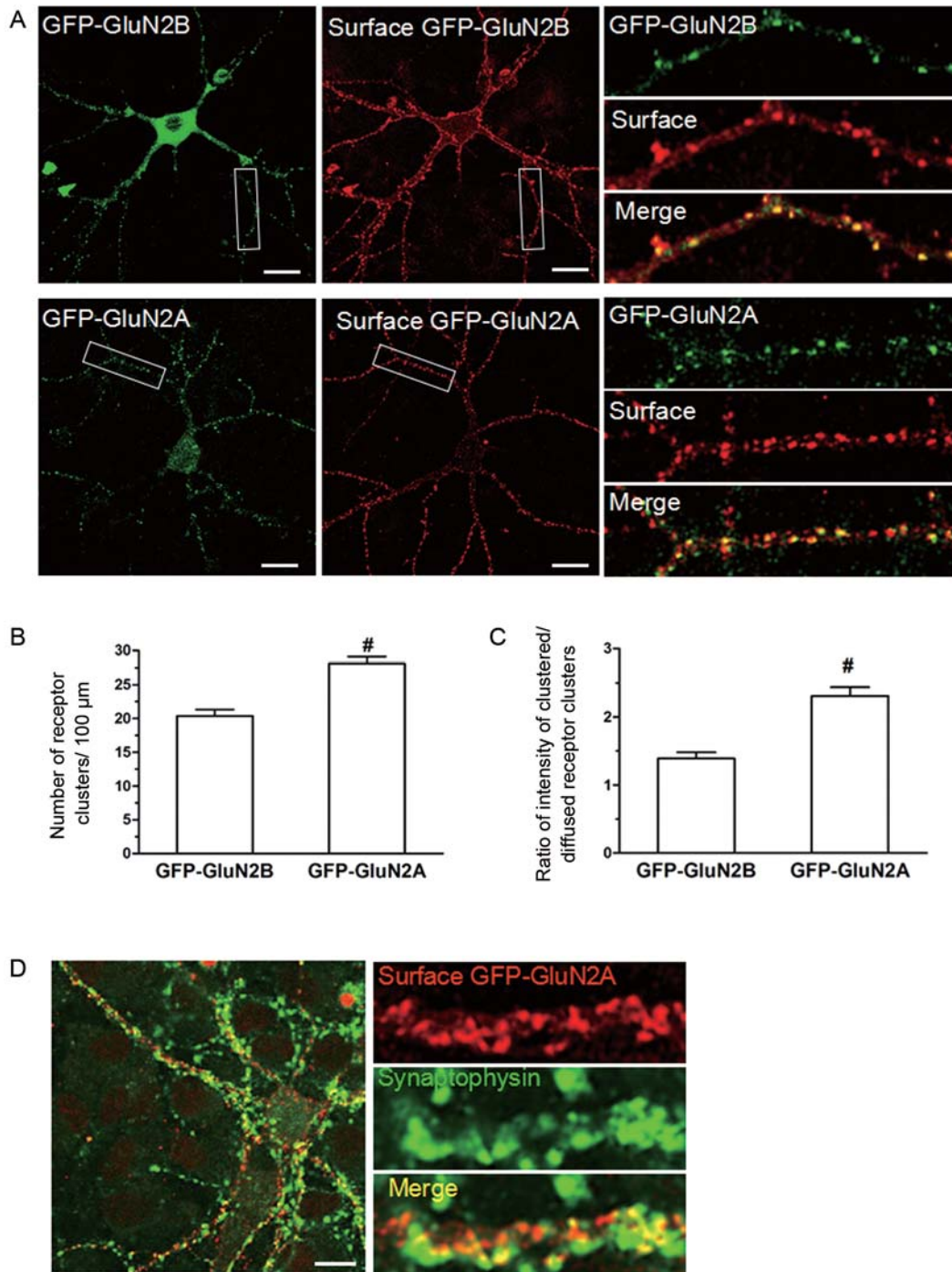


Fig. 2. Distribution patterns of GluN2A- and GluN2B-containing NMDARs at DIV14. **A:** Neurons were transfected with GFP-GluN2A (lower panels) or GFP-GluN2B (upper panels) at DIV5, and then live cell-surface stained with Fab-Cy3 at DIV14 (scale bars, 10 μm). **B:** Density of the surface clusters of GFP-GluN2A or GFP-GluN2B per 100 μm dendrite ([#] $P < 0.01$, Student's t test; mean \pm SEM). **C:** Ratio of average immunofluorescence intensity between the surface clustered and diffuse receptors. The surface NMDARs containing GluN2A or GluN2B were divided into clustered and diffuse pools, and then the ratio of average immunofluorescence intensity of the two pools was measured ([#] $P < 0.01$, Student's t test; mean \pm SEM). **D:** Co-localization of surface NMDARs containing GluN2A (red) and the presynaptic marker protein, synaptophysin (green) at DIV14 after transfection with GFP-GluN2A at DIV5. Most of the surface GluN2A-containing NMDAR clusters were synaptically located at DIV14 ($77.0 \pm 1.9\%$; $n = 20$; scale bar, 10 μm).

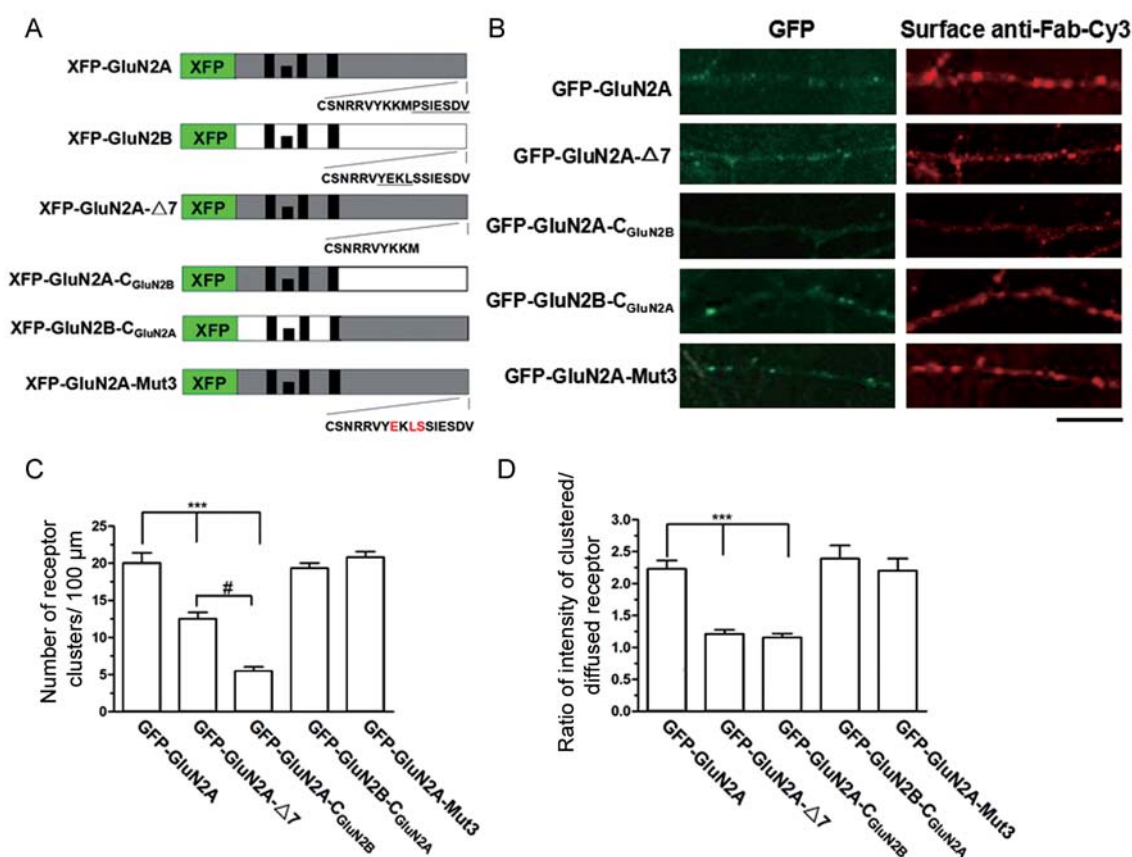


Fig. 3. Surface distribution pattern of GluN2A-containing NMDARs depends on the C-terminus. **A:** Schematic representation of the mutant proteins used in this experiment. XFP indicates GFP or CFP. XFP-GluN2A-Δ7 was a mutation of GluN2A that lacked the last 7 amino-acids (including the PDZ-binding domain). XFP-GluN2A-Mut3 was a mutation of GluN2A, in which the last 11 amino-acids were converted to the corresponding amino-acids in GluN2B (three amino-acids were mutated: K1455E, M1457L, and P1458S). **B:** Hippocampal neurons were transfected with GFP-tagged GluN2A constructs at DIV5, and then were surface-stained with Fab-Cy3 at DIV7 (scale bar, 10 μm). **C:** Number of the surface GluN2A-containing NMDAR clusters per 100 μm dendrite after transfection with different GFP-tagged GluN2A constructs. Compared with full-length GFP-GluN2A, GFP-GluN2A-Δ7 and GFP-GluN2A-C_{GluN2B} showed a decrease in cluster density, while GFP-GluN2B-C_{GluN2A} and GFP-GluN2A-Mut3 did not show a significant difference ($^{***}P < 0.01$, Student's *t* test). More receptor clusters were observed in neurons expressing GFP-GluN2A-Δ7 than in those expressing GFP-GluN2A-C_{GluN2B} ($^{\#}P < 0.05$, Student's *t* test; mean \pm SEM). **D:** Ratio of average immunofluorescence intensity between clustered and diffuse receptors. Compared with full-length GFP-GluN2A, GFP-GluN2A-Δ7 and GFP-GluN2A-C_{GluN2B} showed a decrease in the ratio, while GFP-GluN2B-C_{GluN2A} and GFP-GluN2A-Mut3 did not show a significant difference ($^{***}P < 0.01$, Student's *t* test; mean \pm SEM).

synaptic targeting of NMDARs^[9,18-20]. To assess the role of this domain in the distribution pattern of different NMDAR subtypes, we generated a mutant construct of GluN2A with the last seven amino-acids deleted (GFP-GluN2A-Δ7) (Fig. 3A) and found that the surface density of GFP-GluN2A-Δ7 clusters was significantly lower than that of surface GFP-GluN2A clusters. However, the surface density of GFP-GluN2A-Δ7 clusters was still higher than that of GFP-

GluN2A-C_{GluN2B} clusters (Fig. 3C). This indicated that the PDZ-binding domain of the GluN2A subunit partially determines the distribution pattern of GluN2A-containing NMDARs.

Previous work suggests that YEKL in the distal C-terminus of the GluN2B subunit is a binding site for AP-2, which is pivotal in determining the synaptic localization of GluN2B-containing NMDARs (Fig. 3A). Interestingly, the

GluN2A subunit has a similar motif (YKKM), but this motif is not a substrate for AP-2 binding^[12,19,21]. To determine the role of this motif in the distribution patterns of different NMDAR subtypes, we generated a construct, GFP-GluN2A-Mut3, in which the GluN2A YKKM motif was mutated to YEKL (Fig. 3A). We found that the surface density of GFP-GluN2A-Mut3 clusters did not differ from that of GFP-GluN2A clusters (Fig. 3C), suggesting that the YEKL motif is not important in the determination of NMDAR distribution patterns.

PSD-95 Specifically Associates with Surface GluN2A-containing NMDAR Clusters in Hippocampal Neurons

Our results above indicated that the C-terminus of GluN2 mediates the differential surface distribution pattern between GluN2A- and GluN2B-containing NMDARs. MAGUKs family proteins, including PSD-95 and SAP102, are the major postsynaptic proteins that bind to NMDARs *via* the cytoplasmic tail of the GluN2 subunit. To determine whether association between surface NMDARs and MAGUKs also occurs in a GluN2-dependent manner, we tested the co-localization of MAGUKs (PSD-95 and SAP102) with surface GluN2 subunits (GluN2A and GluN2B). We first co-transfected hippocampal neurons at DIV5 with ECFP-GluN2A or ECFP-GluN2B and PSD-95-GFP and analyzed the co-localization of surface GluN2 clusters with PSD-95-GFP at DIV14 (Fig. 4A, B). We found that most of the surface GluN2B clusters were not concentrated at the sites of PSD-95 puncta, while the surface GluN2A clusters were highly co-localized with PSD-95 puncta (Fig. 4E). Next, we co-transfected cultured hippocampal neurons with SAP102-GFP and ECFP-GluN2A or ECFP-GluN2B, and found that both the surface GluN2B clusters and the surface GluN2A clusters co-localized well with SAP102-GFP (Fig. 4C-E). These data showed that PSD-95, but not SAP102, is specifically associated with surface NMDARs containing GluN2A, indicating that PSD-95 is involved in determining the distribution pattern of different NMDAR subtypes.

Interestingly, the surface density of ECFP-GluN2B clusters was significantly increased when co-expressed with SAP102-GFP (Fig. 4F), suggesting that overexpression of SAP102 induces the clustering of GluN2B-containing NMDARs.

The C-Terminus of GluN2A Determines the Specific Association of Surface GluN2A-containing NMDARs with PSD-95

To identify the structural basis of the specific association of GluN2A with PSD-95, we co-transfected neurons with CFP-GluN2B-C_{GluN2A} or CFP-GluN2A-C_{GluN2B} and PSD-95-GFP (Fig. 5A) and analyzed the co-localization ratios of the surface CFP-GluN2B-C_{GluN2A} or CFP-GluN2A-C_{GluN2B} clusters with PSD-95. We found that the surface GluN2A-C_{GluN2B} was distributed more diffusely and showed little co-localization with PSD-95 puncta. In contrast, surface GluN2B-C_{GluN2A} clusters were highly co-localized with PSD-95 puncta (Fig. 5B). These results indicated that the C-terminus of GluN2 is critical to the different association between NMDAR subtypes and MAGUKs proteins.

Next, we co-transfected neurons with ECFP-GluN2A-Δ7 and PSD-95-GFP, and found that the co-localization level of surface ECFP-GluN2A-Δ7 clusters with PSD-95 was significantly decreased compared to that of surface ECFP-GluN2A with PSD-95 (Fig. 5A). However, it was still higher than the co-localization level of surface GluN2A-C_{GluN2B} with PSD-95 (Fig. 5B). When ECFP-GluN2A-Mut3 and PSD-95-GFP were co-transfected into hippocampal neurons, the surface ECFP-GluN2A-Mut3 clusters co-localized with PSD-95, and did not differ from that of ECFP-GluN2A. Taken together, these data indicated that the PDZ-binding domain of the GluN2A subunit partially determines the specific association of GluN2A-containing NMDARs with PSD-95.

Expression of the GluN2A Subunit Promotes Clustering of PSD-95 in Cultured Hippocampal Neurons

Previous work has shown that the distribution of both endogenous and exogenous PSD-95 protein changes from a diffuse to a clustered pattern in cultured neurons during development^[22]. Here, we also found that PSD-95-GFP was diffusely distributed at DIV7 when transfected alone into cultured hippocampal neurons (Fig. 6A). Interestingly, the density of PSD-95-GFP puncta significantly increased at DIV7 when co-expressed with ECFP-GluN2A, compared with expression alone or co-expression with ECFP-GluN2B (Fig. 6B). Furthermore, PSD-95 puncta were highly co-localized with surface GluN2A-containing NMDAR clusters (Fig. 6C). Together with our finding that overexpression

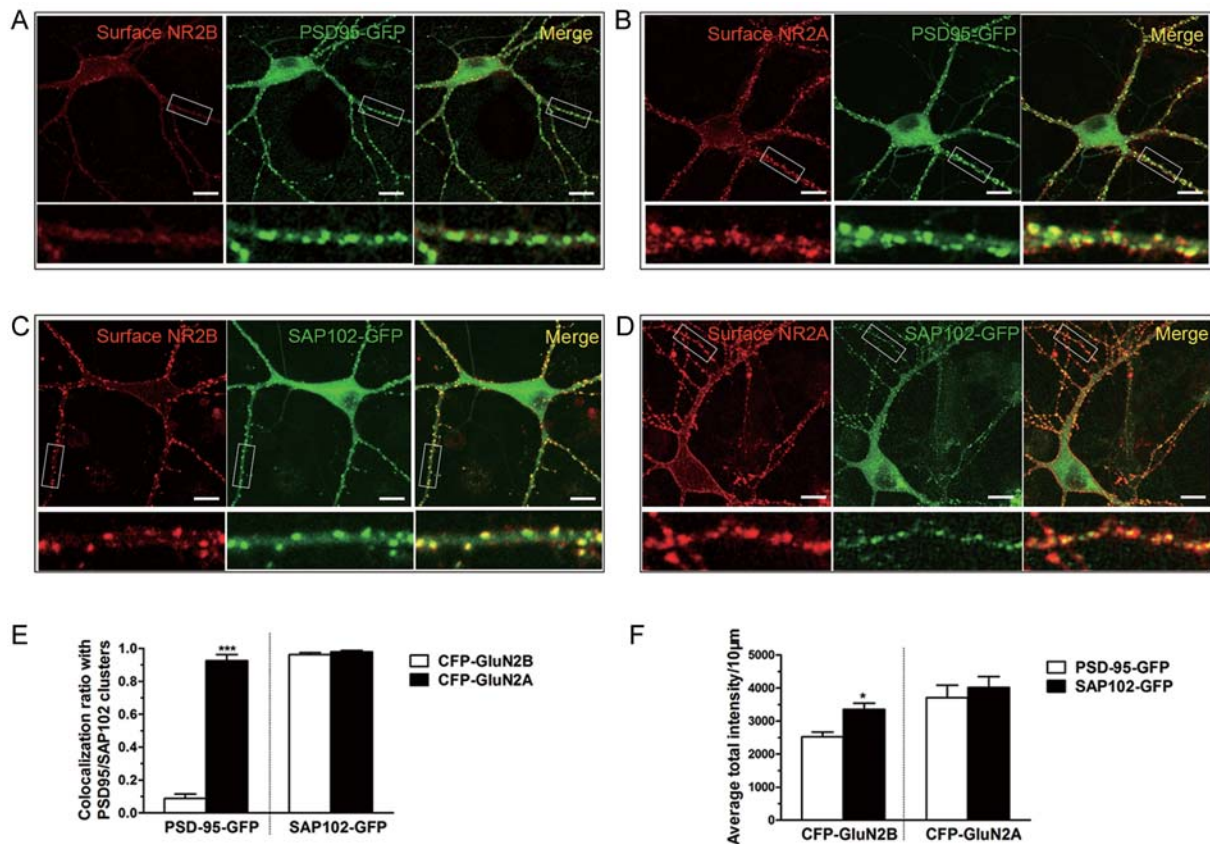


Fig. 4. PSD-95 specifically associates with surface Glu2A-containing NMDARs in hippocampal neurons. A–D: Cultured hippocampal neurons were co-transfected with ECFP-GluN2B/PSD-95-GFP, ECFP-GluN2A/PSD-95-GFP, ECFP-GluN2B/SAP102-GFP, or ECFP-GluN2A/SAP102-GFP at DIV5, and then surface-stained with Cy3-conjugated anti-GFP Fab fragment at DIV14 (scale bars, 10 µm). E: Percentage co-localization of surface-stained GluN2B or GluN2A clusters with PSD-95 or SAP102 puncta. Compared with SAP102, few PSD-95 puncta co-localized with GluN2B-NMDAR clusters (***) $P < 0.01$, Student's t test). As for GluN2A, there were no significant differences in the co-localization ratio with PSD-95 or SAP102 puncta (mean \pm SEM). F: Surface expression levels of GluN2A- or GluN2B-containing NMDARs in neurons co-transfected with PSD-95 or SAP102. The surface expression level of GluN2B-containing NMDARs co-transfected with PSD-95 was lower than after co-transfection with SAP102 (* $P < 0.05$, Student's t test). There were no significant differences in the intensity of surface GluN2A-containing NMDARs in neurons co-transfected with PSD-95 or SAP102 (mean \pm SEM).

of SAP102 induced the clustering of surface GluN2B-containing NMDARs, these results suggested that the distribution pattern of MAGUK proteins or GluN2 subunits is tightly controlled by their expression levels.

DISCUSSION

Previous studies have shown that the GluN2 subunit determines many of the biophysical and pharmacological properties of NMDARs, and also influences NMDAR assembly, downstream signaling, receptor trafficking, and

synaptic localization^[23-25]. In this study, we found that the GluN2 subunit is also responsible for the distinct surface distribution patterns of different NMDAR subtypes. Our results showed that surface NMDARs containing GluN2A were inclined to cluster, while those containing GluN2B were much more diffusely distributed along the dendrites in both immature and mature hippocampal neurons. However, the functional difference between the clustered and the diffuse receptors remains unclear. It is known that receptor clustering is an active process that includes the interaction of receptors with intracellular scaffold proteins,

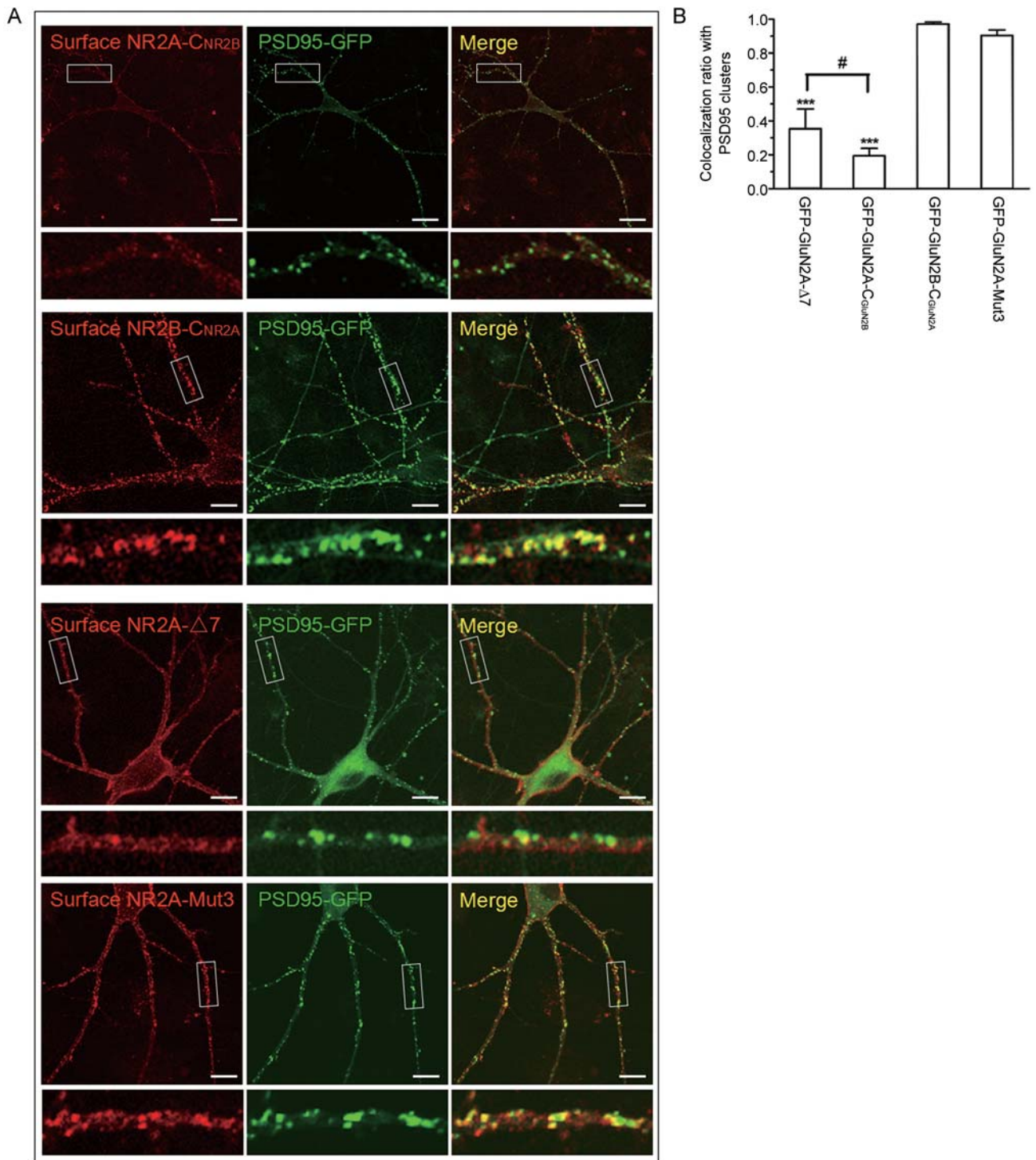


Fig. 5. The PDZ-binding domain partially determines the co-localization of surface GluN2A-containing NMDARs with PSD-95. **A:** Neurons were co-transfected with PSD-95-GFP and different GluN2A mutants, and then surface GluN2A-containing NMDARs were detected with Fab-Cy3 at DIV14 (scale bars, 10 μ m). **B:** Co-localization ratio of surface GluN2A mutant clusters to PSD-95 puncta. Compared with GluN2B-C_{GluN2A}, the co-localization of GluN2A- Δ 7 and GluN2A-C_{GluN2B} with PSD-95 puncta was decreased, while GluN2A-Mut3 showed no statistical difference ($***P < 0.01$, Student's *t* test; mean \pm SEM).

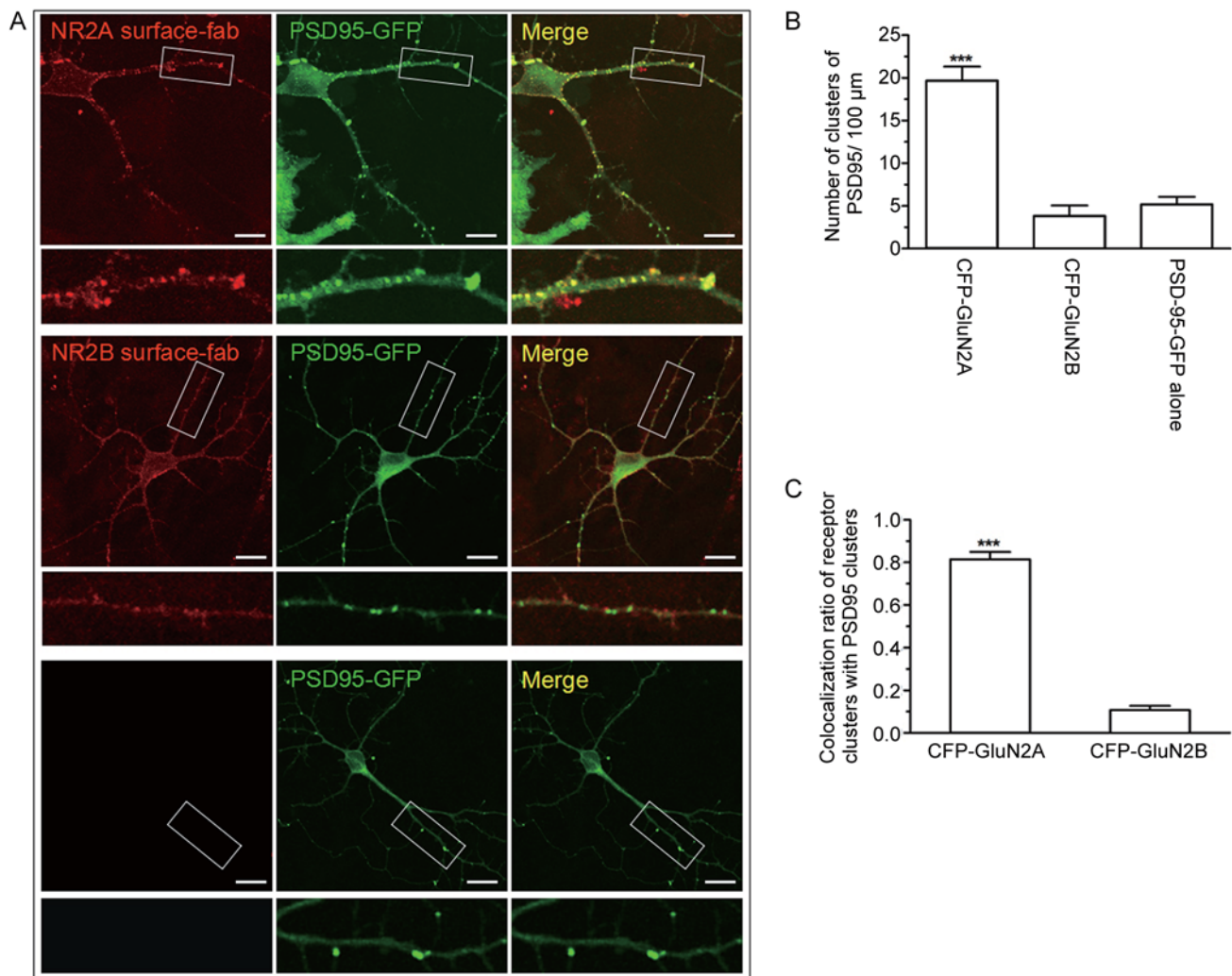


Fig. 6. Overexpression of the GluN2A subunit promotes the clustering of PSD-95 in cultured hippocampal neurons. **A:** Hippocampal neurons were transfected with PSD-95-GFP/CFP-GluN2A (upper panels), PSD-95-GFP/CFP-GluN2B (middle panels), or PSD-95-GFP alone at DIV5 (lower panels), and the distribution pattern of PSD-95-GFP was observed at DIV7 (scale bars, 10 μm). **B:** Number of PSD-95-GFP puncta per 100 μm in different groups. The density of PSD-95-GFP puncta increased when co-transfected with CFP-GluN2A, but not with CFP-GluN2B or expressed alone ($***P < 0.01$, Student's *t* test; mean \pm SEM). **C:** Co-localization ratio of surface receptor clusters with PSD-95 puncta. The co-localization ratio of surface GluN2A-containing receptor clusters with PSD-95 puncta was much higher than that of surface GluN2B-containing receptors ($***P < 0.01$, Student's *t* test; mean \pm SEM).

adaptor proteins, and signaling proteins to form functional complexes. Therefore, the aggregation of neurotransmitter receptors is a central mechanism in neuronal development, synaptic plasticity, and learning. Here, we found that surface GluN2A-NMDARs were clustered even before mature synapses were formed. It is possible that NMDARs containing GluN2A are more important in synaptogenesis than those containing GluN2B. Accordingly, we found

that overexpression of the GluN2A subunit in immature hippocampal neurons induced the clustering of PSD-95, the core component of postsynaptic complexes, which also suggested that expression of the GluN2A subunit promotes the fine-tuning of PSD-95 aggregation. A similar interaction between MAGUK proteins and K^+ channels has been reported. When expressed alone, neuronal MAGUKs or K^+ channels occur diffusely throughout COS cells, while

co-transfection with PSD-95 and Kv_{1.4} results in clustering of both molecules^[26]. Together with our study, these results indicate that the interaction between MAGUK and receptors encourages the formation of functional clusters. Some other studies have reported that receptors within clusters are more stable than those outside of clusters^[27]. Therefore, another possibility is that the surface stability of different NMDAR subtypes is distinct. It may be that the surface NMDARs containing GluN2A do not readily undergo endocytosis, while those containing GluN2B are dynamically exchanged by endocytosis or exocytosis^[28,29].

Our results showed that the entire C-terminus of the GluN2A subunit determines the specific distribution pattern of GluN2A-containing NMDARs, since the patterns were reversed by exchange of the C-termini of the GluN2A and GluN2B subunits. Meanwhile, we found that the PDZ-binding domain of the GluN2A subunit partially, but not completely, determines the clustering of surface NMDARs containing GluN2A. Combined, these data indicate that the interaction of the GluN2 subunits with PSD-MAGUK proteins is one of the key mechanisms for the clustering and synaptic targeting of NMDARs. However, other as yet unknown mechanisms based on the C-terminus of GluN2 are involved in controlling the distribution patterns of surface NMDARs. Recently, research using cultured cortical neurons has shown that the GluN2A and GluN2B subunits have two distinct consensus cysteine clusters in their C-termini. Palmitoylation of these cysteine clusters is involved in the stable expression and constitutive internalization of surface NMDARs^[30]. It will be interesting to explore the role of palmitoylation in the surface distribution patterns of NMDARs.

Previous studies indicate that interactions of the PSD-MAGUK family with NMDARs are subtype-dependent. SAP102 preferentially associates with GluN2B-containing NMDARs, while PSD-95 associates with those containing GluN2A. Another study showed that di-heteromeric GluN1/GluN2A and GluN1/GluN2B receptor populations similarly immunoprecipitate PSD-95, SAP102, and PSD-93 in adult rat hippocampus^[31]. In this study, we found that PSD-95 specifically co-localized with surface NMDARs containing GluN2A, but not those containing GluN2B, which suggests that the specific association of PSD-95 with GluN2A is important for the surface distribution pattern of GluN2A-containing NMDARs.

In summary, here, we have demonstrated that different NMDAR subtypes have distinct surface distribution patterns, which are mainly determined by the C-terminus of the GluN2 subunit. The specific association of PSD-95 with the GluN2 subunit is also critical for the surface distribution pattern and synaptic localization of NMDARs.

ACKNOWLEDGEMENTS

This work was supported by grants from the National Basic Research Program of China (2010CB912002), the National Natural Science Foundation of China (81221003 and 81271453), and Fundamental Research Funds for the Central Universities of China.

Received date: 2014-02-14; Accepted date: 2014-05-12

REFERENCES

- [1] Bliss TVP, Collingridge GL. A synaptic model of memory: long-term potentiation in the hippocampus. *Nature* 1993, 361: 31–39.
- [2] Choi DW, Rothman SM. The role of glutamate neurotoxicity in hypoxic-ischemic neuronal death. *Annu Rev Neurosci* 1990, 13: 171–182.
- [3] Constantine-Paton M, Cline HT, Debski E. Patterned activity, synaptic convergence, and the NMDA receptor in developing visual pathways. *Annu Rev Neurosci* 1990, 13: 129–154.
- [4] Wenthold RJ, Prybylowski K, Standley S, Sans N, Petralia RS. Trafficking of NMDA receptors. *Annu Rev Pharmacol Toxicol* 2003, 43: 335–358.
- [5] Qiu S, Hua YI, Yang F, Chen YZ, Luo JH. Subunit assembly of N-methyl-D-aspartate receptors analyzed by fluorescence resonance energy transfer. *J Biol Chem* 2005, 280: 24923–24930.
- [6] Vicini S, Wang JF, Li JH, Zhu WJ, Wang YH, Luo JH, *et al.* Functional and pharmacological differences between recombinant N-methyl-D-aspartate receptors. *J Neurophysiol* 1998, 79: 555–566.
- [7] Sheng M, Cummings J, Roldan LA, Jan YN, Jan LY. Changing subunit composition of heteromeric NMDA receptors during development of rat cortex. *Nature* 1994, 368(6467): 144–147.
- [8] Ehlers MD. Activity level controls postsynaptic composition and signaling via the ubiquitin-proteasome system. *Nat Neurosci* 2003, 6(3): 231–242.
- [9] Niethammer M, Kim E, Sheng M. Interaction between the C terminus of NMDA receptor subunits and multiple members of the PSD-95 family of membrane-associated guanylate

- kinases. *J Neurosci* 1996, 16: 2157–2163.
- [10] Sprengel R, Suchanek B, Amico C, Brusa R, Burnashev N, Rozov A, *et al.* Importance of the intracellular domain of NR2 subunits for NMDA receptor function *in vivo*. *Cell* 1998, 92: 279–289.
- [11] El-Husseini AE, Schnell E, Chetkovich DM, Nicoll RA, Brecht DS. PSD-95 involvement in maturation of excitatory synapses. *Science* 2000, 290(5495): 1364–1368.
- [12] Lavezzari G, McCallum J, Dewey CM, Roche KW. Subunit-specific regulation of NMDA receptor endocytosis. *J Neurosci* 2004, 24: 6383–6391.
- [13] Zhang XM, Lv XY, Tang Y, Zhu LJ, Luo JH. Cysteine residues 87 and 320 in the amino terminal domain of NMDA receptor GluN2A govern its homodimerization but do not influence GluN2A/GluN1 heteromeric assembly. *Neurosci Bull* 2013, 29(6): 671–684.
- [14] Qiu S, Li XY, Zhuo M. Post-translational modification of NMDA receptor GluN2B subunit and its roles in chronic pain and memory. *Semin Cell Dev Biol* 2011, 22(5): 521–529.
- [15] Luo JH, Fu ZY, Losi G, Kim BG, Prybylowski K, Vissel B, *et al.* Functional expression of distinct NMDA channel subunits tagged with green fluorescent protein in hippocampal neurons in culture. *Neuropharmacology* 2002, 42: 306–318.
- [16] Ishii T, Moriyoshi K, Sugihara H, Sakurada K, Kadotani H, Yokoi M, *et al.* Molecular characterization of the family of the N-methyl-D-aspartate receptor subunits. *J Biol Chem* 1993, 268: 2836–2843.
- [17] Steigerwald F, Schulz TW, Schenker LT, Kennedy MB, Seeburg PH, *et al.* C-Terminal truncation of NR2A subunits impairs synaptic but not extrasynaptic localization of NMDA receptors. *J Neurosci* 2002, 20: 4573–4581.
- [18] Guttman RP, Baker DL, Seifert KM, Cohen AS, Coulter DA, *et al.* Specific proteolysis of the NR2 subunit at multiple sites by calpain. *J Neurochem* 2001, 78: 1083–1093.
- [19] Lavezzari G, McCallum J, Lee R, Roche KW. Differential binding of the AP-2 adaptor complex and PSD-95 to the C-terminus of the NMDA receptor subunit NR2B regulates surface expression. *Neuropharmacology* 2003, 45: 729–737.
- [20] Sans N, Prybylowski K, Petralia RS, Chang K, Wang YX, Racca C, *et al.* NMDA receptor trafficking through an interaction between PDZ proteins and the exocyst complex. *Nat Cell Biol* 2003, 5: 520–530.
- [21] Roche KW, Standley S, McCallum J, Dune Ly C, Ehlers MD, Wenthold RJ. Molecular determinants of NMDA receptor internalization. *Nat Neurosci* 2001, 4: 794–802.
- [22] Craven SE, El-Husseini AE, Brecht DS. Synaptic targeting of the postsynaptic density protein PSD-95 mediated by lipid and protein motifs. *Neuron* 1999, 22: 497–509.
- [23] Tovar KR, Westbrook GL. The incorporation of NMDA receptors with a distinct subunit composition at nascent hippocampal synapses *in vitro*. *J Neurosci* 1999, 19: 4180–4188.
- [24] Stocca G, Vicini S. Increased contribution of NR2A subunit to synaptic NMDA receptors in developing rat cortical neurons. *J Physiol* 1998, 507: 13–24.
- [25] Thomas CG, Miller AJ, Westbrook GL. Synaptic and extrasynaptic NMDA receptor NR2 subunits in cultured hippocampal neurons. *J Neurophysiol* 2006, 95: 1727–1734.
- [26] El-Husseini AE, Topinka JR, Lehrer-Graiwer JE, Firestein BL, Craven SE, *et al.* Ion channel clustering by membrane-associated guanylate kinases. *J Biol Chem* 2000, 275: 23904–23910.
- [27] Bats C, Groc L, Choquet D. The interaction between stargazin and PSD-95 regulates AMPA receptor surface trafficking. *Neuron* 2007, 53: 719–734.
- [28] Besshoh S, Chen S, Brown IR, Gurd JW. Developmental changes in the association of NMDA receptors with lipid rafts yield of lipid rafts increases during postnatal. *J Neurosci Res* 2007, 85(9): 1876–1883.
- [29] Kopp C, Longordo F, Lüthi A. Experience-dependent changes in NMDA receptor composition at mature central synapses. *Neuropharmacology* 2007, 53(1): 1–9.
- [30] Hayashi T, Thomas GM, Haganir RL. Dual palmitoylation of NR2 subunits regulates NMDA receptor trafficking. *Neuron* 2009, 64(2): 213–226.
- [31] Al-Hallaq RA, Conrads TP, Veenstra TD, Wenthold RJ. NMDA di-heteromeric receptor populations and associated proteins in rat hippocampus. *J Neurosci* 2007, 27: 8334–8343.